Determination of a degradation-induced limit for the consolidation of CF/PEEK composites using a thermo-kinetic viscosity model

Olivier de Almeida, Lisa Feuillerat, Jean-Charles Fontanier, Fabrice Schmidt

Determination of a degradation-induced limit for the consolidation of CF/PEEK composites using a thermo-kinetic viscosity model

Olivier De Almeida [a,*], Lisa Feuillerat [a], Jean-Charles Fontanier [b], Fabrice Schmidt [a]

[a] Institut Clément Ader (ICA), Université de Toulouse, CNRS UMR 5312, IMT Mines Albi, UPS, INSA, ISAE-SUPAERO, Campus Jarlard, F-81013 Albi, France
[b] Institut Français du Textile et de l'Habillement (IFTH), 14 rue des Reculettes, 75013 Paris, France

A B S T R A C T

In order to assess the impact of the thermal degradation of PEEK on the consolidation of composite preforms, an impregnation model taking into account degradation is proposed. It includes a viscosity model based on a double Arrhenius law describing the viscosity increase due to degradation. The implementation of this viscosity model into an impregnation model allowed to define an intrinsic processing window for the manufacturing of CF/PEEK composites based on a criterion of irrecoverable viscosity level. The simulation shows a good correlation with the experimentally measured porosity rates of commingled preforms. It predicts the absence of impregnation when increasing the consolidation time or the processing temperature from 380 to 410 °C. Above 410 °C or when increasing the pressure, however, a discrepancy is observed between the model and the simulation. This discrepancy is attributed to a change in the degradation kinetics resulting from a change in oxygen access.

1. Introduction

Because of its melting temperature of 343 °C, the molten state represents a severe condition for Polyether-ether-ketone (PEEK). Therefore, degradation inevitably occurs during processing of long fiber reinforced PEEK matrix composites since PEEK composites are typically processed in the temperature range of 380 to 400 °C.

PEEK degradation mechanisms consist simultaneously in chain cleavage and formation of crosslinks between adjacent aryl groups of polymer chains, and are activated from the rubbery state and above the melting temperature [1–3]. As a consequence of chemical modifications, degradation affects PEEK physical and mechanical properties like the crystallization behavior and the glass transition. It also results in a rapid increase of PEEK viscosity with time due to the dominating effect of crosslinking over chain scission in an oxidant environment [4,5]. Day et al. indeed demonstrated that the atmosphere strongly influences the degradation kinetics. They showed that PEEK was relatively stable in a non-oxidative environment at 400 °C for periods up to 6 h, but that the glass transition temperature and crystallization behavior were rapidly affected under air conditions [6].

As a consequence of the fast degradation kinetics at the molten state, the processability of CF/PEEK composite preforms can be significantly affected. Actually, evidence of degradation due to manufacturing operations of carbon reinforced PEEK composites was already reported [7]. This effect of degradation was for instance observed in a previous study on the consolidation of commingled CF/PEEK preforms [8]. The rapid increase in viscosity of PEEK due to degradation could be correlated with the low level of consolidation obtained under all processing conditions [5]. Phillips et al. also highlighted the impact of degradation on the processability of CF/PEEK composites by analyzing the influence of a preliminary thermal exposure to air of CF/PEEK AS4/APC-2 pre-impregnated tapes on the consolidation behavior [4]. All studies finally conclude that the optimization of CF/PEEK processing conditions consists in finding a compromise between degradation and impregnation kinetics.

However, degradation kinetics are never taken into account when considering the numerical optimization of processing conditions. Numerical approaches, which are usually based on Darcy's law [9] or on the degree of intimate contact [4,10], generally consider a constant Newtonian viscosity that varies with temperature according to an Arrhenius law. As a result, they systematically lead to the definition of processing windows consisting of time and temperature graphs with reciprocal curve shapes of iso-porosity levels [11,12].

Therefore, in order to consider the effect of degradation on the processability of CF/PEEK composites, this study proposes to take degradation into account by means of a thermokinetic model representing the evolution of PEEK viscosity with time. The viscosity model is first described and identified from the experimental shear rheology

* Corresponding author.
E-mail address: olivier.dealmeida@mines-albi.fr (O. De Almeida).

results. This model is then implemented in the impregnation model proposed by Bernet et al. based on Darcy's law to assess the influence of time, temperature and pressure on the consolidation of commingled CF/PEEK composite preforms [13]. The numerical results are finally compared with experimental consolidation data from a previous article [5] in order to analyze the degradation process during consolidation as a function of processing conditions.

2. Materials

The PEEK polymer used as a reference in this study is a Victrex grade 150 provided as a coarse powder (150P). This polymer is characterized by a glass transition of 143 °C and a melting temperature of 343 °C as mentioned in the material's technical data sheet and confirmed by DSC measurements. The composite preform under study is a commingled quadriaxial Non Crimp Fabric (NCF) with a carbon weight fraction of 65%wt. prepared using the same PEEK 150 grade. This NCF preform is composed of four unidirectional layers of an areal weight of 145 $g\,m^{-2}$ stitched together with a PEEK yarn of 5 $g\,m^{-2}$. This corresponds to areal weights Aw_f and Aw_m of 377 $g\,m^{-2}$ and 208 $g\,m^{-2}$ for carbon and PEEK phases respectively. This tailored material was provided by Saertex for the purpose of the INMAT2 project and was manufactured by combining together aligned HTS 3k carbon tows and PEEK yarns so as to obtain a global commingled structure. Because of the alignment of yarns, the commingling level in this material remained poor: no reorganization of PEEK and carbon filaments was performed before the weaving operation. Details about this composite material are given in a previous article [5].

3. Experimental

3.1. Rheological characterization of the matrix

Rheological measurements were performed on PEEK coarse powder and yarns with a Mars Haake rheometer using a plate–plate geometry in oscillatory mode with disposable aluminum plates of a diameter of 35 mm (gap of 1 mm). During the experiments, the shear and shear rates were set to 0.01 and 6.28 s^{-1} respectively. In order to guarantee the linear viscoelastic domain, strain sweep tests were previously performed so that the complex viscosity could be simply determined from the elastic and viscous moduli G' and G''. The applied shear rate is in agreement with the order of magnitude given in the literature in the case of compression molding processes [14–17].

3.2. Consolidation by compression molding

Consolidation of the CF/PEEK preform was performed with a compression molding pilot plant equipped with an induction-heated mold developed by Roctool (3iTech® technology, [18]) following the exact same protocole as in [5]. The laminates were processed with a 200 × 200 mm^2 picture frame at different temperatures comprised between 380 °C and 440 °C during 5 to 30 min and under 25 or 50 bar. All tested experimental conditions are presented in Supplementary data.

A representative processing cycle used for composite consolidation is shown in Fig. 1. The data displayed in Fig. 1 were recorded during the test. It should be noted that the applied force was taken from a load cell in the actuator head of the press and not from the hydraulic pressure, and converted into a pressure by considering the size of the picture frame.

Table 1
Slope of the lines of best fit in Fig. 5 corresponding to factor B in Eq. (4), for each temperature.

Temperature (°C)	Slope (B)
360	1.81
380	2.15
390	2.22
400	2.13
410	1.81
420	1.91

Table 2
Identified parameters of the viscosity model accounting for degradation and reference data of initial viscosity (Eq. (6)) for raw PEEK and PEEK yarns from NCF semi-finished product.

Model parameters	Raw PEEK	PEEK yarn	Unit
T_0	380	380	°C
η_0	355	85	Pa s
E_a	36.4	92.0	kJ mol^{-1}
B	2.0	1.0	s^{-1}
A_0	1.18×10^{14}	4.15×10^{12}	–
E_a^c	267.6	199.6	kJ mol^{-1}

Table 3
Characteristics and material properties used in the impregnation model (Eq. (10)) and for calculating the final void content with Eq. (12).

Abbreviation	Parameter	Value
Model parameters		
R_f	Radius of a single carbon fiber	3.5 µm
r_c	Critical radius	35 µm
Description of the commingled NCF preform		
X_f	Nominal fiber volume fraction	0.58
N_{f_1}	Number of fibers for the first bundle size	3000
ξ_{b_1}	Ratio of the first bundle size	0.5
N_{f_2}	Number of fibers for the second bundle size	6000
ξ_{b_2}	Ratio of the second bundle size	0.5

3.3. Characterization of the final void content of composite plates

Thanks to the picture frame, the flow of resin was constrained into the cavity and squeeze of resin out of the composite stack was avoided. The average laminate thickness t_{lam} of the manufactured laminates could therefore be used as a significant indicator of the porosity level in the composites. The void content ϕ was calculated using Eq. (1), where Aw_f and Aw_m are the areal weights of the carbon reinforcement and the PEEK matrix respectively, ρ_f and ρ_m are the density of carbon fibers and PEEK matrix, set to 1.77 $g\,cm^{-3}$ and 1.30 $g\,cm^{-3}$ respectively according to the manufacturer's data sheets, and n_{plies} corresponds to the number of NCF blankets used to manufacture the composite laminates.

$$\phi = 1 - \frac{n_{plies}}{t_{lam}}\left(\frac{Aw_f}{\rho_f} + \frac{Aw_m}{\rho_m}\right) \quad (1)$$

4. PEEK viscosity modeling including degradation kinetics

4.1. Effect of thermo-oxidation on PEEK viscosity

In order to characterize the influence of temperature on PEEK viscosity and to assess the effects of degradation in the compression molding process, the influence of thermal degradation on the viscous behavior of Victrex PEEK 150 (raw PEEK) and NCF matrix (PEEK yarns) was investigated by measuring the viscosity change with time for different temperatures above PEEK melting temperature. The rheological samples were rapidly heated to a temperature just below the desired temperature so as to avoid temperature overshoot. The PEEK samples were considered as non-degraded at the beginning of the trials.

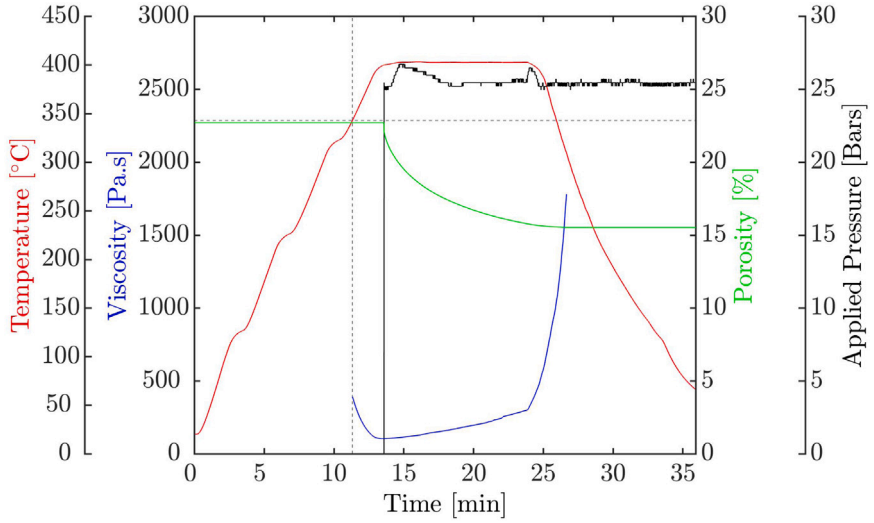

Fig. 1. Processing cycle recorded during the compression molding of 4 plies of CF/PEEK commingled NCF at 400 °C during 10 min under a pressure of 25 bar. The viscosity and porosity are simulated data determined with a rheological model taking into account the degradation behavior of PEEK matrix (Eq. (6)).

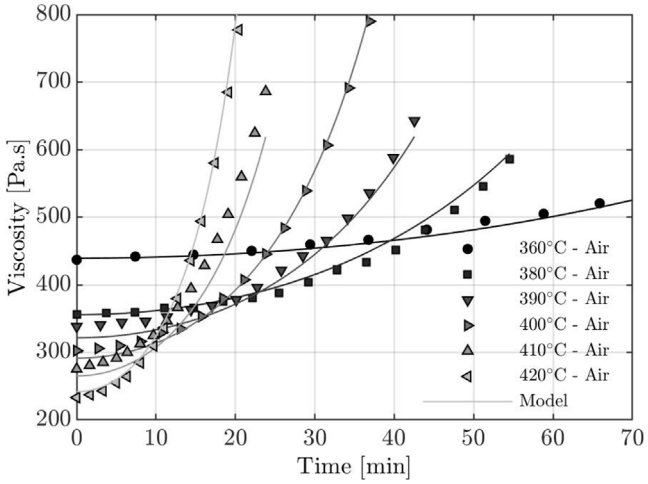

Fig. 2. Comparison of experimental raw PEEK viscosity with the rheological model taking into account the degradation behavior (Eq. (6)).

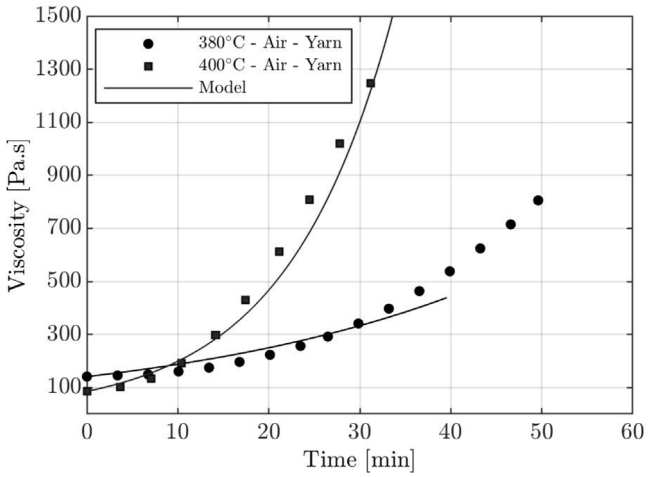

Fig. 3. Comparison of experimental PEEK yarns viscosity (from NCF preform) with the rheological model taking into account the degradation behavior of PEEK yarns (Eq. (6)).

Viscosity measurements of PEEK Victrex 150 coarse powder were carried out for different temperatures between 370 and 420 °C in air (Fig. 2). Due to the difficulty of isolate PEEK filaments from the commingled NCF preforms, only two different temperatures were tested for this PEEK reference (Fig. 3). Indeed, due to the stitched assembly of carbon and PEEK yarns in the NCF preform, PEEK strands had to be extracted one by one until the few grams needed to prepare rheological samples were obtained. The two chosen temperatures are 380 and 400 °C as these are usual processing temperatures for CF/PEEK composites. Higher temperatures could not be used to measure the viscous behavior of PEEK yarns because their fast degradation kinetics [5,8]. Degradation would have rapidly occurred during the heating phase and the test results would not have given accurate information about the actual viscosity.

For both materials, the initial viscosity at $t = 0$ decreases with increasing temperature, which is consistent with the conventional temperature dependence of polymer viscosity. Then, for all temperatures, the viscosity increases rapidly and the viscosity evolution is all the more rapid as the temperature is high above the melting temperature of PEEK. At 420 °C for instance, the increase of raw PEEK viscosity is so rapid that the viscosity is tripled within 18 min. As seen in a previous

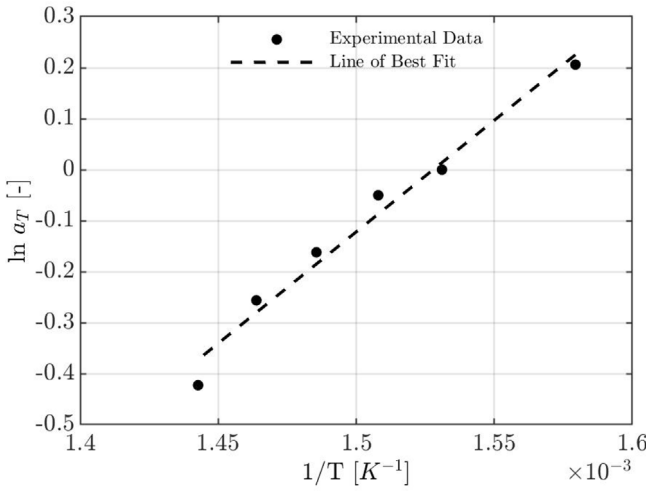

Fig. 4. Arrhenius plot of raw PEEK initial viscosity at $t = 0$. The activation energy of initial viscosity E_a is obtained from the slope of the linear regression according to Eq. (2).

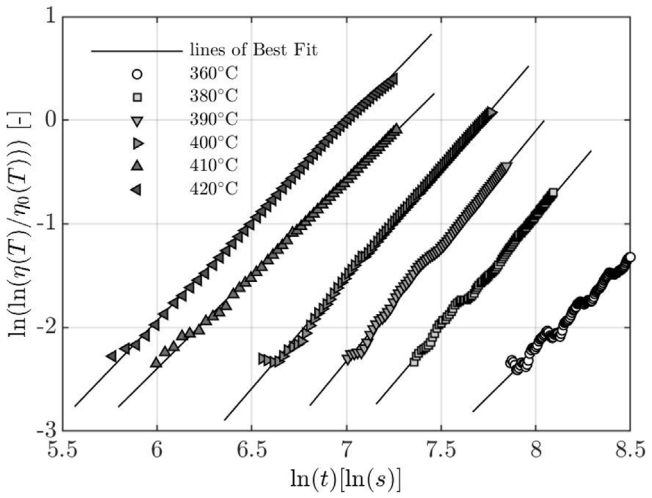

Fig. 5. Double logarithmic plot of normalized raw PEEK viscosity versus the logarithmic of time for different temperatures. The time exponent B in Eq. (4) is given for each temperature by the slopes of the linear regression of experimental data.

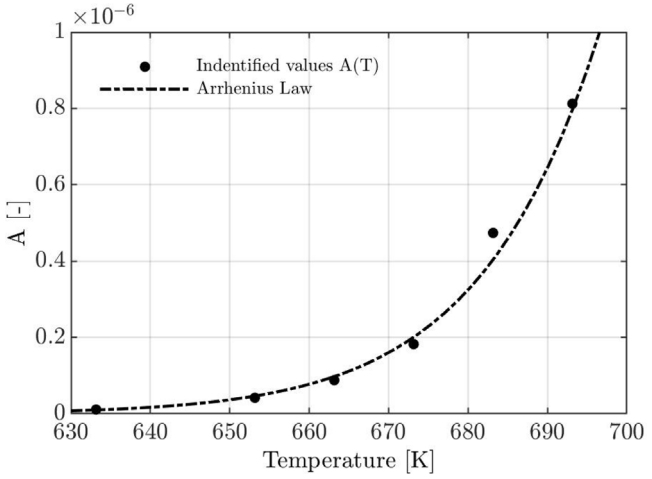

Fig. 6. Kinetic factor $A(T)$ of the viscosity model (Eq. (6)) as a function of temperature for $B = 2$ and comparison with the prediction given by the Arrhenius law of Eq. (5).

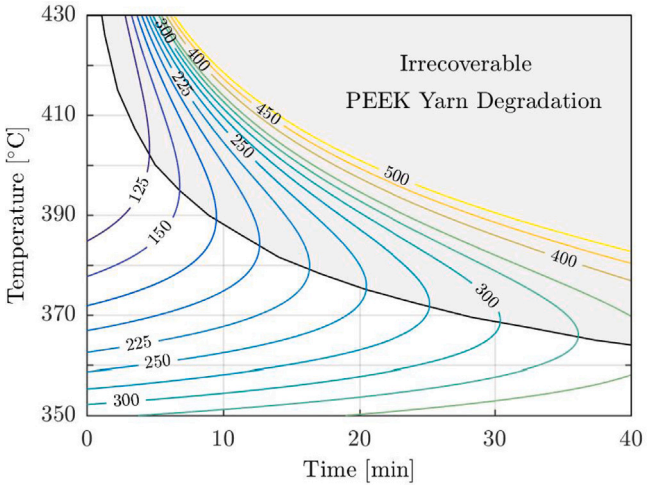

Fig. 7. Iso-viscosity contours computed with the viscosity model accounting for degradation (Eq. (6)) using material parameters identified from viscosity measurements on PEEK yarns (Table 2). The black curve connecting the maximum time of each iso-viscosity level defines a limit of irrecoverable degradation.

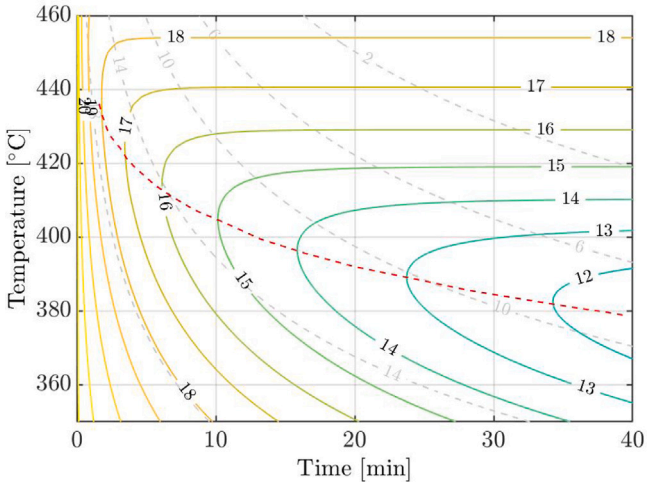

Fig. 8. Iso-porosity contours computed with Bernet's impregnation model (Eqs. (10) and (12)) for a consolidation pressure of 25 bar using material parameters identified from viscosity measurements on PEEK yarns (Table 2). Dashed gray lines represent the iso-porosity levels considering the temperature dependency of initial viscosity but without considering degradation kinetics (Eq. (2)); colored lines are obtained using the viscosity model accounting for degradation (Eq. (6)). The red line connecting the minimum time of each iso-porosity contour defines the processing window for impregnation.

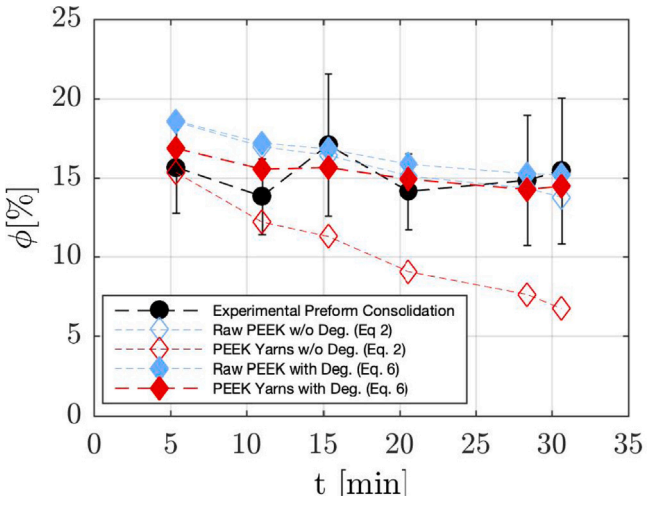

Fig. 9. Comparison of the experimental void contents resulting from processing conditions of 400 °C and 25 bar (•) with the predictions obtained with the viscosity model when considering only the temperature dependence (Eq. (2) without degradation, ◊) and when taking into account degradation in addition (Eq. (6), ◆). The blue symbols (◊) correspond to the simulation performed with the parameters identified for the pure matrix, the red symbols (◊) for the PEEK yarns from the preform. Dotted lines are shown to indicate trends.

article [5], filaments from NCF preform have a lower initial viscosity than raw PEEK but degrade much faster. This effect is attributed to the presence of the sizing deposited at the surface of extruded PEEK yarns in the melt spinning process before drawing. The sizing limits the friction of polymer yarns on the drawing godets and allows yarns manipulation for further winding and weaving operations. The low degradation temperature of this sizing however accelerates PEEK degradation mechanisms. As a consequence, the viscosity of PEEK filaments triples in less than 25 min at 400 °C, while it requires more than 40 min for obtaining an equivalent change with raw PEEK.

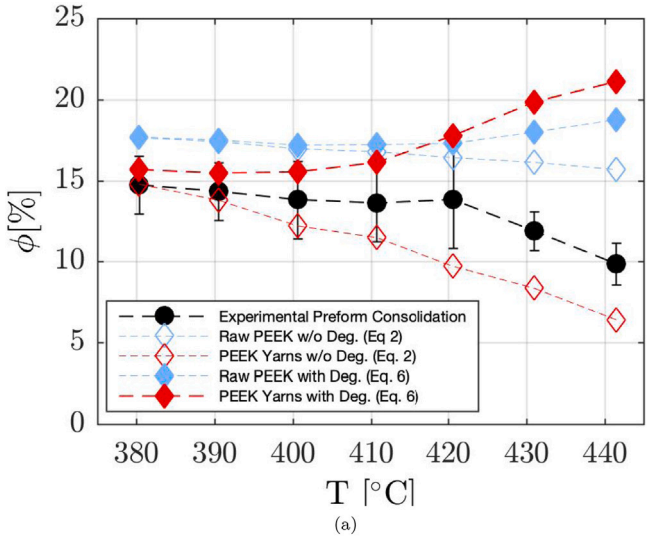

(a)

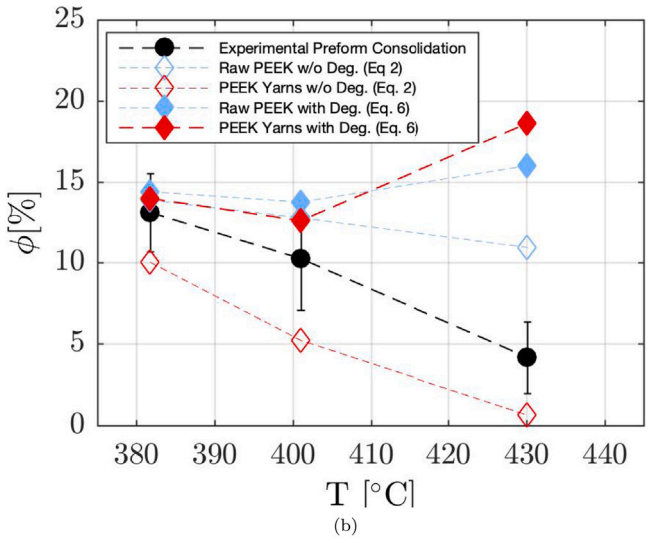

(b)

Fig. 10. Comparison of the experimental void contents resulting from processing conditions of (a) 10 min and 25 bar and (b) 20 min and 50 bar (•) with the predictions obtained with the viscosity model when considering only the temperature dependence (Eq. (2) without degradation, ◊) and when taking into account degradation in addition (Eq. (6), ♦). The blue symbols (◊) correspond to the simulation performed with the parameters identified for the pure matrix, the red symbols (◊) for the PEEK yarns from the preform. Dotted lines are shown to indicate trends.

4.2. Raw PEEK viscosity modeling

To further analyze the effect of degradation, a viscous model accounting for degradation kinetics was developed. The aim of this model is to predict the viscosity change over time for any temperature above the melting temperature.

First, as already noticed, the thermal dependency of the initial viscosity at $t = 0$ is in good agreement with the conventional behavior of thermoplastic polymers, and therefore can be modeled using an Arrhenius law. The viscosity at $t = 0$, $\eta_0(T)$, was modeled with Eq. (2), where a_T is the shift factor, E_a is the Arrhenius activation energy, R is the gas constant and T_0 is a reference temperature (380 °C in the present study). As shown in Fig. 4, the alignment of the data points in the chart of $ln(a_T)$ vs. $1/T$ confirms the Arrhenius type for the thermal sensitivity of initial viscosity. The identified activation energy is 36372 J mol^{-1}, which is in agreement with values given in literature

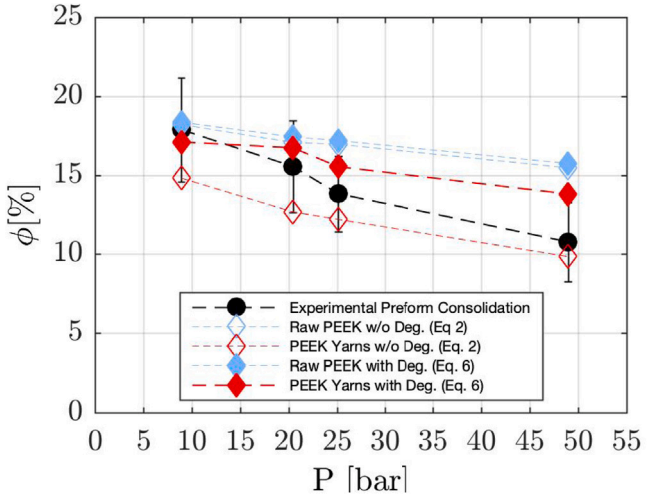

Fig. 11. Comparison of the experimental void contents resulting from processing conditions of 400 °C and 10 min (•) with the predictions obtained with the viscosity model when considering only the temperature dependence (Eq. (2) without degradation, ◊) and when taking into account degradation in addition (Eq. (6), ♦). The blue symbols (◊) correspond to the simulation performed with the parameters identified for the pure matrix, the red symbols (◊) for the PEEK yarns from the preform. Dotted lines are shown to indicate trends.

for the viscosity of PEEK grade 150 [19,20].

$$\eta_0(T) = \eta_0(T_0)a_T = \eta_0(T_0)\exp\left(\frac{E_a}{R}\left(\frac{1}{T} - \frac{1}{T_0}\right)\right) \tag{2}$$

As PEEK degradation is a kinetic phenomena, the degradation kinetics is usually described as an exponential function of time t in viscosity models. Analytical models predicting an exponential change in viscosity have already been proposed by Phillips et al. and Malkin et al. [4,21]. In a first approach, the temperature dependence of degradation kinetics was thus described with Eq. (3), where $A(T)$ is a parameter that depends only on the temperature.

$$\eta(t,T) = \eta_0(T)\exp\left(A(T)t\right) \tag{3}$$

As shown in Fig. 5, the plot of $\ln(\ln(\eta(T)/\eta_0(T)))$ vs. $\ln(t)$ exhibits straight lines which means that degradation kinetics can be modeled by an exponential of the product of two factors respectively depending on time and temperature. However, contrary to previous studies, the linear regression over the $\ln(t)$ domain gives slope values different of unity. A power of time is therefore required to accurately model the time dependent behavior of PEEK viscosity. An exponent coefficient B was therefore added to Eq. (3) to obtain Eq. (4). This time exponent B reflects the sensitivity of the degradation to time and is therefore indirectly related to the kinetic constants of the chemical degradation reactions. However, the degradation mechanisms are governed by about ten reactions and it is therefore not possible to establish a direct relationship between the exponent and the kinetic constants.

$$\eta(t,T) = \eta_0(T)\exp\left(A(T)t^B\right) \tag{4}$$

Table 1 summarizes the $B(T)$ values for the different temperatures. As it can be seen, they are comprised between 1.81 and 2.22, with no apparent temperature dependency and it was decided in a first approximation to use the mean value of the slopes i.e. 2.00 for coefficient B in Eq. (4). To improve the model definition for A, the $A(T)$ coefficients were recalculated for each temperature considering the mean value of B, i.e. $B = 2$. This was achieved simply by re-identifying the intercept of the line of best fit with the y-axis in Fig. 5 specifying the exponent $B = 2$. Fig. 6 shows the temperature dependency of recomputed coefficients A.

Here again, the variation of A with temperature is consistent with an exponential function of the reciprocal of temperature. Considering

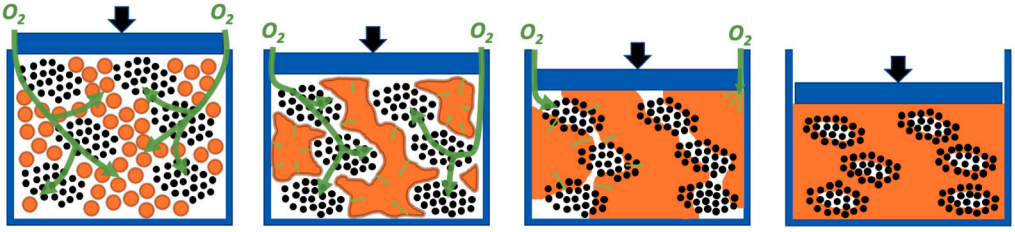

Fig. 12. Schematic representation of oxygen transport within a composite preform during compression molding processing.

the chemical crosslinking process that is responsible of this change, a chemical based Arrhenius law is thus proposed to model $A(T)$ according to Eq. (5). In the same way as for $A(T)$ and B coefficients, the pre-exponential factor A_0 and the activation energy E_a^c in Eq. (5) could be identified by means of a linear regression on the plot of $log(A)$ versus the reciprocal of temperature.

$$A(T) = A_0 \exp\left(\frac{-E_a^c}{RT}\right) \tag{5}$$

As shown in Fig. 6, the Arrhenius law accurately predicts the variation of A with temperature. The identified values for the pre-exponential factor A_0 and the activation energy E_a^c are respectively 1.18×10^{14} and 267.6 kJ mol^{-1}. This value of activation energy is in agreement with the literature [19].

The proposed model finally allows determining the variation of PEEK viscosity with time and temperature from a reference of initial viscosity $\eta_0(T_0)$ with only 4 parameters (Eq. (6)): the activation energy of the relaxation process (E_a), the activation energy of the thermally activated chemical degradation process (E_a^c) and two constants A_0 and B. As it can be noticed in Fig. 2, the predicted values of viscosity are in good agreement with the experimental degradation kinetics: the model accurately predicts the initial viscosity as well as the increase in viscosity over time.

$$\eta(t,T) = \eta_0(T_0) \exp\left(\frac{E_a}{R}\left(\frac{1}{T} - \frac{1}{T_0}\right)\right) \exp\left(A_0 \exp\left(\frac{-E_a^c}{RT}\right) t^B\right) \tag{6}$$

4.3. Viscosity of PEEK yarns from NCF

The same procedure was applied for the identification of the model parameters for PEEK yarns in order to predict their viscosity during the consolidation of the semi-finished product. The comparison of the experimental viscosity data with the model is displayed in Fig. 3. Although the model does not agree as well with the experimental data as in the case of raw PEEK, a good correlation is observed up to 40 min of isotherm for PEEK yarns. Since the consolidation of NCF semi-finished products has been studied experimentally up to 30 min of isothermal plateau, the model prediction, nevertheless, remains accurate in a processing window from 0 to 40 min.

All identified model parameters, i.e. E_a, E_a^c, A_0 and B, and reference data $\eta_0(T_0)$ for PEEK yarns and raw PEEK are summarized in Table 2. The same reference temperature of $T_0 = 380\ °C$ was chosen in the Arrhenius law of initial viscosity for both materials (Eq. (2)). The activation energy identified for the initial viscosity E_a is significantly higher in the case of PEEK yarns than for raw PEEK. This can be explained by the presence of sizing on the surface of the extruded yarns which has relatively low thermal stability [8]. At low temperatures, the yarn sizing provides a lubricating effect that lowers the initial viscosity, but this effect vanishes at higher temperatures due to sizing degradation. The other parameters that are involved in the description of the degradation kinetics (Eqs. (4) and (5)) are also significantly different between the two PEEK references. The identification of the exponent B for the PEEK yarns led to a value of B=1. The model formulation used for PEEK yarns is therefore similar to the model previously proposed in literature [4,21]. Nevertheless, the activation energy E_a^c related to crosslinking kinetics is lower for the PEEK filaments than for raw PEEK, which indicates that less energy is required to degrade PEEK yarns than the raw PEEK. This is consistent with the experimental rheology measurements showing that the temperature has a stronger effect on the viscosity increase for PEEK yarns than for raw PEEK. Here again, this can be attributed to the presence of the sizing solution on the surface of the extruded PEEK yarns. The high temperature sensitivity of the sizing accelerates degradation kinetics as the temperature increases.

5. Impregnation model accounting for PEEK degradation

In order to predict the advancement of commingled preform consolidation, the viscosity model taking degradation into account was implemented in the impregnation model proposed by Bernet et al. [13]. In this way, it was possible to predict the final porosity content of the composite plates manufactured with the studied commingled preform.

5.1. Bernet's impregnation model for commingled yarns

The impregnation model developed by Bernet et al. [13] is a two-dimensional model specifically proposed for modeling the consolidation of commingled preforms. This section summarizes the main assumptions and equations of this approach. For further information on this model, the reader is invited to refer to the corresponding article detailing the approach developed by these authors.

The main assumption of Bernet's model is that all commingled yarns in a preform are geometrically equivalent and undergo impregnation simultaneously. The model is therefore based on a description of a commingled preform by means of a representative unit element, which is the commingled yarn. Once the matrix is melted, the commingled yarn is assumed to be constituted of dry fibers surrounded by the matrix bed under pressure. In order to account for the size distribution of the dry fiber bundles, different populations of fiber bundles are considered in the description of the commingled preform.

The initial state of a dry fiber bundles from a population i is defined by its radius r_0^i that is defined with Eq. (7) in which R_f corresponds to the radius of an elementary fiber ($R_f = 3.5$ µm is considered in this study for carbon fibers), v_f is the fiber volume fraction in dry fiber bundles and N_f^i is the number of fibers in the fiber bundle.

$$r_0^i = \sqrt{\frac{N_f^i R_f^2}{v_f}} \tag{7}$$

The molten matrix is considered as a fluid of constant viscosity and impregnation is described using Darcy's Law (Eq. (8)), where u_l and u_s are respectively the local velocities of matrix and fibers, K_P is the permeability tensor within fiber bundles which depends on v_f, η the viscosity and P the local pressure.

$$(1 - v_f)(u_l - u_s) = \frac{-K_P}{\eta} \nabla P \tag{8}$$

Only a flow orthogonal to the fibers is considered and the fiber bed is assumed compressed to a constant value of v_f. Thus, $u_s = 0$ and K_P is constant. By resolving the simplified Darcy's law (Eq. (9)) and assuming mass conservation, Eq. (10) is obtained.

$$(1 - v_f)u_l = (1 - v_f)\frac{dr_i}{dt} = \frac{-K_P}{\eta}\frac{\partial P}{\partial r} \tag{9}$$

$$\frac{dr_i}{dt} = \frac{K_P}{\eta(1-v_f)r_i \ln\left(\frac{r_i}{r_0^i}\right)}(P_c + P_a - P_g) \tag{10}$$

In Eqs. (9) and (10), $r_i(t)$ is the front flow at time t, P_c is the capillary pressure which is here neglected, P_a is the applied pressure during the consolidation and P_g is the gas pressure at the front flow. When, $r_i \geq r_c$, P_g is equal to atmospheric pressure and for $r_i < r_c$ the gas law applies and yields $P_g = P_{atm}\left(\frac{r_c}{r_i}\right)^2$, where r_c is the unimpregnated bundle radius below which the pore is closed. In the present study, the same value that was proposed by Bernet et al. for this critical radius r_c was used, i.e. 35 μm.

5.2. Application to commingled NCF consolidation

As described in a previous paper [5], the semi-finished product is composed of yarns that are more juxtaposed than actually commingled. The commingled structure of the preform is thus assumed to be composed of populations of yarns of different sizes. Two populations were considered (Table 3): a population of 3k carbon yarns referring to isolated carbon yarns surrounded by PEEK filaments and a population of two 3k yarns, i.e. composed of 6000 carbon filaments, that corresponds to a situation of two juxtaposed carbon yarns in the preform. Then, since the proportion of one population to the other was difficult to assess in a stack of NCF preforms, it was supposed that the probability of the two situations was equivalent. A bundles fraction ξ_b of 50% for each population was thus taken into account for the simulation of the consolidation of the commingled NCF preforms.

The fiber volume fraction in dry fiber bundles v_f is a parameter that depends on the pressure applied to the fibrous preform. It is usually determined by means of compression tests. In the present case, the commingled preform does not allow the determination of this parameter in a simple way. As proposed by Bernet et al. [13], the v_f values were thus adjusted according to the pressure applied to the preform during consolidation considering low temperature and short processing conditions for which degradation could be considered negligible. For pressures below 15 bar, v_f was set to 0.762, between 15 and 20 bar v_f was 0.767, between 20 and 25 bar v_f was 0.768 and above 45 bar v_f was 0.769. These values are in good agreement with the values proposed by Bernet et al. and logically reflect the increase in fiber content with the pressure.

The viscosity η was calculated through the previously proposed model, which takes into account the degradation phenomenon. In order to assess the PEEK behavior during the total consolidation process, the model was used to simulate the change in viscosity during thermal cycles representative of the compression molding process. As the viscosity model is explicit, the differential form of Eq. (6) was used to calculate the change in viscosity during isothermal as well as for non-isothermal time increments Δt. The viscosity was simulated with Eq. (11), where $\dot{T}$ is the heating or cooling rate during the time increment Δt. The viscosity parameters identified for the PEEK yarns that are summarized in Table 3 were used for the simulation of the commingled NCF preform consolidation.

$$\begin{aligned}\eta(t,T(t)) =& \eta(t-\Delta t, T(t-\Delta t)) + \frac{d\eta(t,T(t))}{dt}\Delta t \\ =& \eta(t-\Delta t, T(t-\Delta t)) \\ &+ \Delta t\left[\eta_0(T_0)\exp\left(\frac{E_a}{R}\left(\frac{1}{T}-\frac{1}{T_0}\right)\right)\exp\left(A_0\exp\left(\frac{-E_a^c}{RT}\right)t^B\right)\cdots\right. \\ &\left.\left(\frac{-E_a}{RT^2}\dot{T} + \frac{A_0E_a^c}{RT^2}|\dot{T}|\exp\left(\frac{-E_a^c}{RT}\right)t^B + A_0\exp\left(\frac{-E_a^c}{RT}\right)Bt^{B-1}\right)\right]\end{aligned} \tag{11}$$

5.3. Assessment of void content

From the calculated radius $r_i(t)$ of a bundle of each population, is was possible to compute the macroscopic void ratio ϕ from the cross-sectional areas of the fiber bundles in m^2 according to Eq. (12), where A_v, A_f and A_m are the areas associated with voids, fibers and matrix respectively in the 2D representation of the commingled material, defined by Eqs. (13), (14) and (15) respectively.

$$\phi = \frac{A_v}{A_v + A_f + A_m} \tag{12}$$

$$A_v = (1-v_f)\sum_{i=1}^{n}\xi_{b_i}\pi(r_i)^2 \tag{13}$$

$$A_f = \pi R_f^2\sum_{i=1}^{n}\xi_{b_i}N_{f_i} \tag{14}$$

$$A_m = \frac{(1-X_f)}{X_f}A_f \tag{15}$$

In Eqs. (13) and (14), ξ_{b_i} corresponds to the bundle fraction of the population i, X_f is the fiber volume fraction determined from the areal weights and densities of fiber and matrix in the NCF preform and N_{f_i} is the number of carbon fibers in a commingled bundle of the population i (Table 3).

6. Simulated viscosity and porosity features

Fig. 7 shows the iso-viscosity contours for PEEK yarns calculated in the temperature range above the melting temperature using the viscosity model. For all viscosity levels, the iso-viscosity contours show a particular maximum time with a vertical asymptote that defines a change in the viscous behavior. Whatever the initial temperature, the change in viscosity due to thermo-oxidation can be counterbalanced by gradually increasing the temperature up to this particular point. However, beyond this maximum time, the advancement of degradation no longer allows the same level of viscosity to be maintained. The viscosity of the polymer is no longer recoverable and necessarily increases with time. The curve connecting the maximum value of time of each viscosity level therefore represents a natural limit to PEEK flowability that is independent of the preform characteristics and processing conditions.

By plotting the iso-porosity curves from the impregnation model for a pressure of 25 (Fig. 8), the boundary of irrecoverable PEEK degradation domain transforms into a processability limit. Like the iso-viscosity curves, the iso-porosities show vertical asymptotes and the curve connecting the corresponding times represents a dramatic change in the impregnation behavior.

For short times and/or low temperatures, the effect of degradation is moderate and the porosity level decreases progressively over time. In this range of processing conditions, the iso-porosities appear as reciprocal time curves similar to those described in the literature [4, 12] as this is η_0 that controls impregnation. The iso-porosity curves calculated when ignoring the degradation parameters (with Eq. (2)) are indeed almost perfectly superimposed at low temperature with the model taking into account degradation (Eq. (6)).

However, the two models diverge progressively as the processability limit defined from the vertical asymptotes is approached, due to the intensification of degradation at high temperature. Indeed, this theoretical processing limit is beyond the limit of irrecoverable PEEK degradation (Fig. 7) and impregnation is already critically affected by the increase in viscosity of the matrix. Therefore, beyond this boundary, for a given temperature, the porosity ratio no longer decreases because of the limited flowability of the matrix.

Increasing the consolidation pressure from 25 bar to 50 bar does not broaden the processability window since the processability limit directly arises from the viscosity model. Simply, the levels of porosity that can be obtained before reaching the processability limit are lower due to the application of higher pressure. Under 50 bar, the model

predicts a minimum of 9%vol of porosity which is far too high for expecting the material to satisfy aerospace requirements. For the same reason, considering a different degree of commingling by changing the size distribution of the fiber bundles has no effect on the position of the processability limit. According to the model, only a higher pressure would allow reducing further the final porosity ratio. Also, whatever the processing conditions, the lowest porosity ratio that can be obtained within 40 min corresponds to a processing temperature of 380 °C. According to the impregnation model accounting for degradation, this condition therefore represents an optimal setting for the consolidation of the NCF preform.

7. Model comparison with experimental consolidation data

7.1. Time evolution of viscosity and porosity

Thanks to the thermo-kinetic viscosity model and impregnation model, the change in viscosity and porosity evolution could be computed for each processing condition. The actual temperature and pressure recorded during consolidation by the pilot plant were used to be representative of the experimental conditions. Fig. 1 shows an example of a consolidation cycle with simulated viscosity and porosity. The viscosity and resulting impregnation level were computed during the entire cycle when PEEK is in the molten state, i.e. from 343 °C during the heating phase and until 310 °C during the cooling phase. These temperatures were chosen as they correspond to PEEK melting and crystallization temperatures. Nevertheless, the transition temperature has little impact on the simulation results since PEEK viscosity is too high in the transition range of temperature for allowing resin flow whatever the degradation kinetics.

During the heating phase, the viscosity first decreases because the degradation kinetics are slower than the effect of temperature on the initial viscosity $\eta_0(T)$. The viscosity then increases throughout the isothermal plateau due to degradation, and this increase intensifies during cooling because the thermo-dependent and degradation effects on the viscosity are cumulative. The consequences on the porosity ratio also depend on the pressure and no porosity evolution thus occurs during the heating phase. Capillary effects could have slightly modified the porosity level during the heating phase, but their contribution is estimated to be of the order of a few kPa [22] and have therefore been neglected in this study. With the application of the consolidation pressure, the porosity rate decreases rapidly until it gradually stabilizes to the final value. The slowdown in impregnation results from the increase in viscosity due to degradation in combination with the effect of temperature during cooling.

Figs. 9–11 compare the experimental porosity ratios with the final void content given by the simulations after the cooling phase. The value of t_{lam} used in Eq. (1) for the determination of the experimental void content is the average of 13 thickness measurements taken at locations on the plates that are representative of their thickness. The error bars displayed for the experimental data represent the variability in porosity content resulting from variation in thickness measurements on compression molded laminates.

Different configurations of the viscosity model were considered for the comparison: based on the viscosity of raw PEEK or on that of PEEK yarns, and with or without taking degradation into account. This last condition then corresponds to classical modeling approaches proposed in literature [4,12].

7.2. Influence of consolidation time

Fig. 9 shows the void content as a function of the isothermal stage duration for a processing temperature of 400 °C and a pressure of 25 bar. Whatever the temperature, the preform consolidation systematically led to a high void content of about 15%. Contrary to what could be expected, increasing the consolidation duration did not result in a lower void content. This is the direct consequence of degradation and was already discussed in a previous article [5]. As the degradation level and crosslinking effect increase with time, the use of longer consolidation times does not improve impregnation and the porosity ratios remain stable. Nevertheless, it must be noticed that a benefit of consolidation time could be observed for a processing temperature of 430 °C under 50 bar (see Supplementary data).

The porosity ratios predicted with the impregnation model based on PEEK yarns viscosity are in good agreement with experimental results. The viscosity model therefore well describe the effect of consolidation time on degradation and impregnation. For this temperature, the simulations based on NCF matrix show lower porosity ratios than those based on raw PEEK up to 20 min. This is due to the lubricating effect of yarns sizing that lowers PEEK initial viscosity and benefits to impregnation [5]. The consideration of degradation particularly affects PEEK yarns behavior that exhibit fast degradation kinetics at this temperature. Increasing the isotherm time from 5 to 30 min only reduces the void content from 17% down to 14.5%, while it is decreased to 7% when degradation is dismissed. For raw PEEK, taking degradation into account has little effect on the porosity ratio: crosslinking kinetics is moderate at this temperature.

7.3. Influence of temperature

The consequence of PEEK degradation appears even more clearly in Fig. 10 that shows the results for a 10 min isotherm under 25 bar and for a 20 min isotherm under 50 bar. When plotting porosity ratios as a function of the processing temperature, the impregnation model predicts that an increase in the processing temperature results in a higher porosity ratio because of the higher degradation kinetics. According to the simulated data, the influence of degradation becomes predominant beyond 410 °C which indicates that degradation can be detrimental to consolidation at high temperature.

The influence of temperature on experimental porosity data however does not follow the prediction. Instead, for a consolidation pressure of 25 bar, the porosity level remains constant whatever the processing temperature up to 420 °C and decreases when using higher temperatures. This non-linear effect of temperature does not fit Darcy's description of impregnation, whether or not degradation is considered by viscosity. Other phenomena may therefore be activated beyond a temperature level, with a potential interaction with degradation mechanisms.

This non linearity of the porosity level with temperature vanishes under a consolidation pressure of 50 bar. Under high pressure, the porosity level decreases with temperature over the whole range of temperature. Again, neither viscous model conditions fit with experimental data, but contrary to 25 bar, the evolution of porosity follows the trend given by the impregnation model based on the initial viscosity η_0 although experimental porosity ratios are higher than the ones obtained from the simulation.

7.4. Influence of pressure

The influence of pressure on porosity is finally presented in Fig. 11. It appears that for low consolidation pressures, the impregnation model accounting for degradation well predicts the porosity content. However, as it was suggested by the difference in consolidation behavior between Figs. 10(a) and 10(b), it can be seen that the higher the pressure, the less degradation affects impregnation. Degradation thus seems to have moderate effect on consolidation when using high pressures as if it is hindered when consolidation is rapid.

8. Discussion

Due to their high transition temperatures, high performance polymers such as PEEK undergo irreversible chemical changes at high temperature that alter their behavior. Because of its glass transition of 143 °C, these chemical reactions are activated in the rubbery state [3], but their effect is rapidly noticeable when increasing the temperature above PEEK melting temperature in an oxidative environment. The chemical reactions responsible for the degradation of PEEK result in an increase in molar mass due to crosslinking of PEEK macromolecules [1,2,6,23–25] and therefore in a rapid increase in the melt viscosity.

The porosity levels determined after processing the commingled NCF CF/PEEK preforms confirm that the increase in viscosity due to degradation affects impregnation when processing high performance thermoplastic composite laminates. Increasing the duration of the isothermal stage or increasing the processing temperature from 380 to 410 °C has indeed almost no effect on consolidation. These results are in good agreement with the results of Phillips et al. who studied the effect of exposing PEEK films to high temperature on the consolidation of CF/PEEK composites [4]. In this time–temperature domain, this effect of degradation on the porosity content is well described by the impregnation model taking degradation into account. This is the domain in which iso-porosity curves start diverging from the prediction based on the initial viscosity $\eta_0(T)$. This domain corresponds to processing conditions beneath the processability limit defined on the iso-porosity diagrams.

The model however lacks in predicting the porosity ratios when using processing temperatures above 410 °C or using a pressure of 50 bar. The processing conditions influence the porosity of laminates according to the model based on $\eta_0(T)$, as if degradation is no longer effective under severe processing conditions. The theoretical processability limit that is based on the impregnation model accounting for degradation is thus misnamed: the results of NCF preform consolidation indeed suggest that despite the risk of degrading PEEK matrix the use of very high processing temperatures and pressure may be beneficial for impregnation.

The modification of degradation kinetics also suggests that a kinetic factor is changed beyond a temperature and pressure threshold. Several factors can affect PEEK degradation kinetics, the additives being one of them. The difference in viscous behavior between raw PEEK and PEEK from NCF yarns was actually attributed to the presence of sizing [5,8]. However, it is unlikely that the change in impregnation kinetics is due to a rapid volatilization of the chemical additives at high temperature without inducing degradation. According to the degradation mechanisms, the main factor that can significantly modify crosslinking kinetics is the presence of oxygen. Many studies actually reported comparisons of degradation kinetics as a function of the atmosphere environment, and oxygen is definitively involved in the degradation mechanisms as a reactive species [3,6]. The most logical explanation for the discrepancy between experimental and simulation results is therefore that oxygen availability is different when consolidation is achieved at high temperature and high pressure.

Oxygen transport to the PEEK matrix results from two main mechanisms of different kinetics that are schematically described in Fig. 12: convection and diffusion. This transition has actually been demonstrated by Zhang et al. in their study of the out-of-autoclave consolidation of CF/PEEK pre-impregnated tapes [26]. At the beginning of consolidation, the porosities in the melted commingled preform form channels that allow oxygen convection throughout the composite material. Oxygen diffusion is then negligible as regards to the diameter of PEEK filaments or the size of the liquid bed formed by the melted yarns around carbon fiber bundles. But, as impregnation progresses, the open porosities within the composite preform gradually turn into closed porosities. Oxygen convection is no longer possible and the oxygen concentration in the matrix phase then mainly depends on oxygen diffusion through the composite length and/or thickness. Since diffusion is a much slower process than convection, the availability of oxygen to PEEK, i.e. the local concentration in the composite material, is rapidly reduced, which certainly slows down degradation kinetics. Therefore, according to this process, the moment the oxygen supply process within the composite material change from a convection-driven to a diffusion-driven process is crucial, because the earlier it occurs, the less degradation affects impregnation.

Regardless of degradation, the higher the processing temperature and the applied pressure, the faster the impregnation according to Darcy's law. Indeed, the low initial viscosity η_0 at high temperature above 420 °C as well as a high consolidation pressure ($P_a > 50$ bar) induces a rapid reduction of the porosity ratio before degradation is too advanced. The temperature and pressure threshold in iso-porosity diagrams may thus represent a limit beyond which impregnation is fast enough for obtaining a composite microstructure of closed porosities before degradation has affected PEEK viscosity to a critical level.

In addition to the balance between diffusion and convection, the matrix degradation can influence oxygen diffusion. Indeed, by analyzing the property gradient that appears over time through the thickness of PEEK samples subjected to an oxidizing atmosphere at high temperature above 400 °C, Pascual et al. [27] demonstrated that PEEK degradation kinetics are the result of the balance between oxygen diffusion and temperature-dependent reaction kinetics. They concluded that the different kinetics of both processes lead to the formation of a highly oxidized layer at the surface of samples exposed to temperatures higher than 400 °C. Using a high temperature or a high pressure can therefore be even more beneficial as the degradation of the composite surface can concentrate degradation and preserve the sample core.

However, if the impregnation behavior in CF/PEEK laminates depends on oxygen concentration and the balance between convection and diffusion processes within PEEK matrix, this means the viscosity measurements were also affected with the existence of a gradient of degradation kinetics throughout the radius of the rheology samples during the experiments. The periphery of the cylindrical samples was probably faster degraded than the sample core because of the air flow within the rheometer oven while the sample core was preserved from oxygen and thus from degradation. A thorough investigation of the viscous behavior of PEEK matrix is therefore required for a better representation of the actual behavior of PEEK filaments in a composite preform. To do so, a dimensionless viscous model would be useful in order to consider the actual behavior of a PEEK matrix whatever its shape factor in the composite preform.

9. Conclusions

In order to better describe the influence of degradation on CF/PEEK composite manufacturing, a viscosity model was developed based on rheological tests. This model well predicts the change in viscosity of raw PEEK and PEEK yarns from NCF matrix that is induced by the crosslinking mechanism. The double Arrhenius exponential law is only based on 4 parameters, two Arrhenius constants and two pre-exponential factors. The Arrhenius constants express the thermal dependence respectively of the non-degraded viscosity and the crosslinking formation kinetics.

The viscosity model allowed proposing an intrinsic processability criterion for PEEK. This processing limit is simply based on the impossibility after a certain time to counterbalance the viscosity change by increasing the temperature. It differs from the other processing limits available in literature in that it is independent of impregnation parameters.

By implementing the viscosity model into the impregnation model developed by Bernet et al. for commingled preforms, the model demonstrated its ability to describe degradation effects. The discrepancy of simulation results with experimental data at high temperature and pressure however indicates that the degradation process is not continuous over the entire consolidation process. The change of oxygen availability from the moment closed porosities are formed is the most probable assumption for explaining the lack of model prediction at high temperature and pressure.

CRediT authorship contribution statement

Olivier De Almeida: Conceptualization, Methodology, Software, Investigation, Writing – original draft, Writing – review & editing, Supervision. **Lisa Feuillerat:** Investigation, Visualization, Writing – original draft, Writing – review & editing. **Jean-Charles Fontanier:** Resources, Writing – review & editing. **Fabrice Schmidt:** Supervision, Project administration.

Declaration of competing interest

The authors declare the following financial interests/personal relationships which may be considered as potential competing interests: Olivier De Almeida reports financial support was provided by Région Occitanie.

Acknowledgment

The authors wish to thank the Region Occitanie for their financial support.

Appendix A. Supplementary data

Supplementary material related to this article can be found online at https://doi.org/10.1016/j.compositesa.2022.106943.

References

[1] Jonas A, Legras R. Thermal stability and crystallization of poly(aryl ether ether ketone). Polymer 1991;32(15):2691–706.
[2] Day M, Sally D, Wiles DM, Chemistry D. Thermal degradation of poly(aryl-ether-ether-ketone) : Experimental evaluation of crosslinking reactions. J Appl Polym Sci 1990;40(30271):1615–25.
[3] Courvoisier E, Bicaba Y, Colin X. Multi-scale and multi-technique analysis of the thermal degradation of poly(ether ether ketone). Polym Degrad Stab 2018;151:65–79.
[4] Phillips R, Glauser T, Månson JAE. Thermal stability of PEEK/carbon fiber in air and its influence on consolidation. Polym Compos 1997;18(4):500–8.
[5] Feuillerat L, De Almeida O, Fontanier J-C, Schmidt F. Effect of poly(ether ether ketone) degradation on commingled fabrics consolidation. Composites A 2021;149:106482.
[6] Day M, Suprunchuk T, Cooney JD, Wiles DM. Thermal degradation of poly(aryl-ether-ether-ketone) (PEEK): A differential scanning calorimetry study. J Appl Polym Sci 1988;36(28274):1097–106.
[7] Dolo G, Férec J, Cartié D, Grohens Y, Ausias G. Model for thermal degradation of carbon fiber filled poly(ether ether ketone). Polym Degrad Stab 2017;143:20–5. http://dx.doi.org/10.1016/j.polymdegradstab.2017.06.006.
[8] De Almeida O, Feuillerat L, Nouri V, Choquet K. Influence of composite preform fabrication on the integrity of poly-aryl-ether-ketone matrices. J Appl Polym Sci 2021;138(30):1–15.
[9] Bernet N, Michaud V, Bourban PE, Manson JAE. Commingled yam composites for rapid processing of complex shapes. Composites A 2001;32(11):1613–26.
[10] Lee WI, Springer GS. A model of the manufacturing process of thermoplastic matrix composites ifacture. J Compos Mater 1987;21:1017–55.
[11] Hou M, Ye L, Leeb HJ, Maib YW. Manufacture of a carbon-fabric-reinforced polyetherimide (CF / PEI) composite material. Compos Sci Technol 1998;58:181–90.
[12] Ye L, Friedrich K, Kästel J, Mai YW. Consolidation of unidirectional CF/PEEK composites from commingled yarn prepreg. Compos Sci Technol 1995;54(4):349–58.
[13] Bernet N, Michaud V, Bourban P-E, Manson J-AE. An impregnation model for the consolidation of thermoplastic composites made from commingled yarns. J Compos Mater 1999;33:751–72.
[14] Seo JW, Lee W. A model of the resin impregnation in thermoplastic composites. J Compos Mater 1991;25(9):1127–42.
[15] Jespersen ST, Wakeman MD, Michaud V, Cramer D, Månson JA. Film stacking impregnation model for a novel net shape thermoplastic composite preforming process. Compos Sci Technol 2008;68(7–8):1822–30.
[16] Gebart BR. Permeability of unidirectional reinforcements for RTM. J Compos Mater 1992;26(8):1100–33.
[17] Choupin T, Fayolle B, Régnier G, Paris C, Cinquin J, Brulé B. Macromolecular modifications of poly(etherketoneketone) (PEKK) copolymer at the melting state. Polym Degrad Stab 2018;155:103–10.
[18] Ramakrishnan KR, Le Moigne N, De Almeida O, Regazzi A, Corn S. Optimized manufacturing of thermoplastic biocomposites by fast induction-heated compression moulding: Influence of processing parameters on microstructure development and mechanical behaviour. Composites A 2019;124:105493.
[19] Khan MA, Mitschang P, Schledjewski R. Identification of some optimal parameters to achieve higher laminate quality through tape placement process. Adv Polym Technol 2010;29(2):98–111.
[20] Shekar RI, Damodhara Rao P, Siddaramaiah, Padaki V, Kim NH, Lee JH. Fibre-fibre hybrid composites for aerospace applications. Adv Mater Res 2010;123–125:1231–4.
[21] Malkin AY, Kulichikhin SG. Rheokinetics of curing. Adv Polym Sci 1991;101:216–57.
[22] Michaud V, Mortensen A. Infiltration processing of fibre reinforced composites: Governing phenomena. Composites A 2001;32(8):981–96.
[23] Day M, Cooney JD, Wiles DM. The thermal stability of poly(aryl-ether ether-ketone) as assessed by thermogravimetry. J Appl Polym Sci 1989;38(29850):323–37.
[24] Day M, Cooney JD, Wiles DM. The thermal degradation of poly(aryl-ether-ether-ketone) (PEEK) as monitored by pyrolysis-GC/MS and TG/MS. J. Analytical and Applied Pyrolysis 1990;18(31856):163–73.
[25] Cole KC, Casella IG. Fourier Transform infrared spectroscopic study of thermal degradation in films of poly(etheretherketone). Thermochim Acta 1992;211:209–28.
[26] Zhang D, Heider D, Gillespie JW. Design and optimization of oven vacuum bag (OVB) processing for void air removal in high-performance thermoplastic composites. J Thermoplast Compos Mater 2020. http://dx.doi.org/10.1177/0892705720978248.
[27] Pascual A, Toma M, Tsotra P, Grob MC. On the stability of PEEK for short processing cycles at high temperatures and oxygen-containing atmosphere. Polym Degrad Stab 2019;165:161–9.